

# Minority carrier lifetime in silicon wafers and thin-film material

Philipp Rosenits, Fraunhofer Institute for Solar Energy Systems (ISE), Freiburg, Germany

## ABSTRACT

The minority carrier lifetime is a key parameter for the performance of solar cells as it characterizes the electrical quality of the semiconductor material. Consequently, accurate and reliable methods to determine the minority carrier lifetime are of enormous interest for both practical process control and the evaluation of the potential and limitations of a specific cell concept. Due to its importance, many different lifetime measurement techniques have been developed and used over the past few decades. This paper aims to present and discuss the most common measurement methods on the one hand, while attempting to shed light on some recent developments on the other. The determination of the minority carrier lifetime of crystalline silicon thin-film (cSiTF) material is illustrated as an example of interest for those who are already familiar with standard lifetime characterization.

## Introduction

Each photon that impinges on the surface of a solar cell or its predecessor, typically a 150–200 $\mu\text{m}$ -thick silicon wafer acting as the solar cell's starting material, will either be reflected at the front surface or enter the bulk of the cell. Roughly 75 to 90% of all incoming photons from the terrestrial solar spectrum are absorbed by a 150 $\mu\text{m}$ -thick solar cell (the precise fraction depends on the applied light trapping mechanisms such as anti-reflection coating, front- or back-side texturing, etc.). Virtually every absorbed photon generates an excess charge carrier pair, consisting of an excess electron and excess hole. After some time, these excess carriers disappear again, a process known as recombination. The characteristic time of this process is called excess (or minority) carrier lifetime. If the excess carriers manage to reach the front and back contacts of the solar cell within their lifetime, i.e. before they recombine, they are then of use for power generation by the solar cell; otherwise they are lost. Therefore, the higher the lifetime, the better the solar cell's performance, all other factors being equal.

**“The higher the lifetime, the better the solar cell's performance, all other factors being equal.”**

The minority carrier lifetime in silicon wafers destined for photovoltaic applications can vary by several orders of magnitude. Common silicon solar cell materials exhibit lifetimes between 1 $\mu\text{s}$  and a few milliseconds. However, for 1 $\mu\text{m}$ -thick polycrystalline silicon thin-film material, for instance, a few nanoseconds may be sufficient to reach acceptable cell performance. On undoped silicon

wafer material, on the contrary, lifetimes exceeding 100ms have been measured [1].

The impact of the lifetime on the device performance is twofold. On the one hand, the lifetime influences the extractable voltage of the solar cell. As a very rough estimate (assuming basically an injection-independent minority carrier lifetime, low-level injection and negligible contact resistances), the relationship between lifetime and voltage is logarithmic. For typical standard solar cells, an increase of the lifetime by a factor of 10 improves the device performance by approximately 10% (an assumption based on a calculation of the implied open circuit voltage of a 1 $\Omega\text{cm}$  p-type solar cell with a minority carrier lifetime of 50 $\mu\text{s}$  under 1 sun illumination).

On the other hand, the cell's output current is also related to the lifetime. Since the minority carriers need some time to diffuse from their place of generation to the *p-n* junction (and ultimately to the contacts), a higher lifetime enhances the charge collection probability and thus improves the extractable current of the solar cell.

In steady-state conditions, as is the case for thermal equilibrium or constant illumination, the rates of carrier generation and recombination are perfectly balanced. For an undoped semiconductor in equilibrium, the population of free charge carriers is given by the so-called intrinsic carrier concentration  $n_i$ , which is in the range of  $10^{10}\text{cm}^{-3}$  charge carriers for silicon at room temperature; for doped material the majority carrier density equals the concentration of ionized dopants  $N_{\text{Dop}}$  and the minority carrier density adjusts to  $n_i^2/N_{\text{Dop}}$ . Under illumination, additional electrons and holes are generated in the semiconductor material. The density of these excess charge carriers  $\Delta n$  depends on the minority carrier lifetime  $\tau$  and the net generation rate  $G$ , which itself

depends on the incoming photon flux and its spectral distribution, the front surface reflectance and the thickness of the sample.

$$\Delta n = G \times \tau \quad (1)$$

For example, if a typical 150 $\mu\text{m}$ -thick silicon wafer with a standard anti-reflection coating at the front surface and a minority carrier lifetime of 50 $\mu\text{s}$  is illuminated by strong sunlight (having an intensity, or irradiance, of  $100\text{mW}/\text{cm}^2$  and the standard spectral distribution of AM1.5g), a steady-state excess carrier concentration of  $\Delta n = 7 \times 10^{14}\text{cm}^{-3}$  is established in the sample, greatly exceeding the intrinsic carrier concentration. Standard industrial-type solar cells operate in the range of  $\Delta n = 1 \times 10^{13} - 1 \times 10^{15}\text{cm}^{-3}$ , while high-efficiency silicon solar cells can reach  $\Delta n = 1 \times 10^{16}\text{cm}^{-3}$  under operating conditions. Cells under concentrated sunlight may even exceed this value, and crystalline thin-film solar cells sometimes operate below  $\Delta n = 1 \times 10^{13}\text{cm}^{-3}$ .

The injection-dependent lifetime, giving a so-called lifetime curve, for a typical silicon wafer in photovoltaics is depicted in Fig. 1. One very important feature becomes immediately apparent from the graph: the value of the minority carrier lifetime is strongly affected by the range of the excess carrier density considered, also known as the injection level. Therefore, when reporting lifetime results, the corresponding injection level must always be included. Up to this point, reference has been made to a value called carrier lifetime, which in a real sample is determined by several individual recombination processes that occur simultaneously and independently of each other. The only accessible measurement quantity in lifetime measurements is therefore a so-called effective lifetime  $\tau_{\text{eff}}$ , illustrated in red in Fig. 1.

Fab & Facilities

Materials

Cell Processing

Thin Film

PV Modules

Power Generation

Market Watch

The different recombination channels, which all bring their individual injection dependence into the game, include intrinsic recombination, which takes place radiatively from band to band or occurs by means of a third charge carrier (Auger recombination). Additionally, an electron-hole pair can recombine via defect levels due to impurity atoms or crystallographic imperfections of the crystal lattice, which is summarized in the term Shockley-Read-Hall (SRH) recombination. Finally, recombination can take place at the surfaces, usually quantified by a surface recombination velocity or saturation current density or expressed in terms of a fictive surface lifetime. The inverse sum of all these individual lifetimes  $\tau_i$  leads to the inverse effective lifetime:  $1/\tau_{\text{eff}} = \sum_i 1/\tau_i$ . Via careful selection of the investigated injection level range, selected recombination processes can be studied explicitly, e.g. Auger recombination at high-level injection or SRH recombination at low-level injection, if the surfaces are well passivated.

### Lifetime measurement techniques

There are two basic approaches to measuring the lifetime in silicon wafers. One method involves maintaining a steady-state generation of known value in the sample under investigation (e.g. by constant illumination), measuring the excess carrier density and hence calculating the lifetime. An alternative is to terminate the generation abruptly and measure the rate at which the excess carrier density diminishes. The former

method is referred to as the steady-state method, the latter the transient decay method. For both cases, the following equation applies for the determination of the minority carrier lifetime [2].

$$\tau_{\text{eff}}(\Delta n) = \frac{\Delta n(t)}{G(t) - \frac{d\Delta n(t)}{dt}} \quad (2)$$

Transient decay methods are attractive because they only rely on the relative change of the carrier density with time and no additional geometric, electrical and optical sample properties (such as thickness, doping concentration, carrier mobilities, front surface reflectance, etc.) are required – which makes the determination of the lifetime relatively simple and robust. Although it is not strictly required, it is highly advisable to monitor the excess carrier density level at which the measurement takes place as a reported lifetime is only meaningful in conjunction with a specified injection level. If the lifetime depends strongly on the excess carrier density in the investigated range, a determination of the lifetime by transient decay measurements is not straightforwardly possible; however, an indicative value obtained without knowledge of the injection level is frequently found to be a useful quality measure.

In steady-state lifetime measurements, the generation rate needs to be known quite accurately. This means in practice that for every sample, the amount of photons that are absorbed within the sample has to be determined. Once

the generation rate is determined, the injection level can easily be calculated. A modification of the steady-state method consists of quasi-steady-state lifetime measurements, where the excitation light intensity is substantially varied (typically up to three orders of magnitude) during the measurement with a time constant that is large compared to the lifetime of the investigated material. This method is powerful, as usually a whole injection-dependent lifetime curve is obtained within a few measurements. However, an accurate determination of the generation rate is still required.

**“There exist transient, steady-state and quasi-steady-state lifetime measurement techniques.”**

The spatial information that can be deduced from lifetime measurements varies considerably. Some techniques only provide a very rough spatial resolution in the range of centimetres; other methods yield a higher resolution in the millimetre and micrometre range, but spatial information of the whole wafer requires time-consuming scanning. Finally, a fast method to obtain spatially-resolved lifetime results is available by camera-based measurement techniques, where high resolution images of large sample areas can be obtained within seconds.

Table 1 presents some measurement techniques for determining the minority carrier lifetime in silicon material destined for photovoltaic applications, including three important features of the methods regarding lifetime measurements. Firstly, there is the possibility of determining injection-dependent lifetimes. It should be noted that in principle, steady-state and transient lifetime measurement methods can also provide injection-dependent lifetime curves by simply repeating the measurement for a set of different illumination intensities. With regard to measurement time and precision, this is, however, not comparable with quasi-steady-state measurement methods, where hundreds or thousands of lifetime values at different injection densities are obtained within one single measurement.

The second and third features depicted in Table 1 are the measurement mode and spatial resolution of each method, respectively. Methods that are in widespread use and techniques that have been recently developed have been selected and included, although this is not an exhaustive list and many other interesting methods exist in addition to those named in the table.

Photoconducance decay methods, and

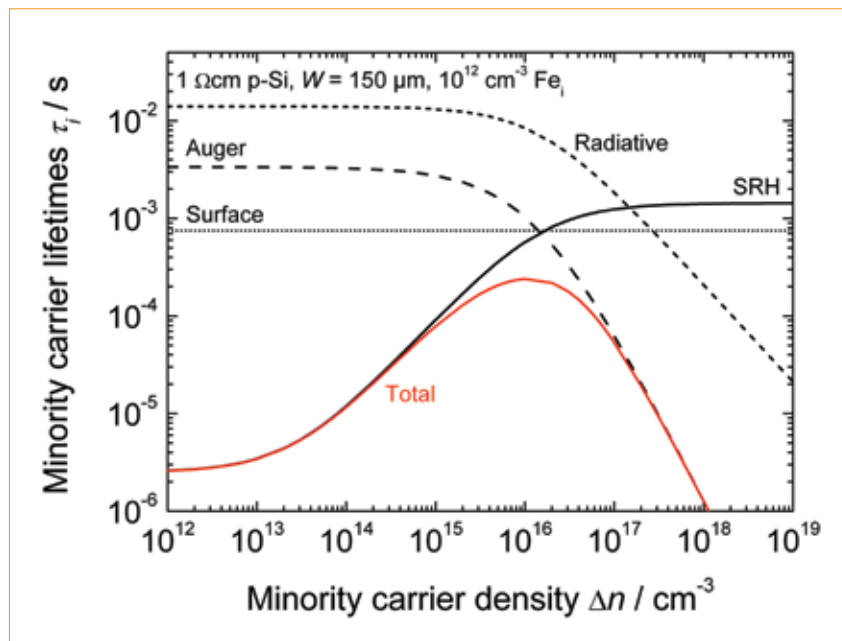


Figure 1. Simulation of the influence of different recombination channels. For silicon material, radiative and Auger recombination are typically only relevant for high minority carrier densities. Shockley-Read-Hall (SRH) recombination is modelled by  $10^{12}\text{cm}^{-3}$  interstitial iron atoms in this example; an injection-independent surface recombination of  $S = 10\text{cm/s}$  has been assumed.

Method	Injection-dependence of lifetime?	Time domain/ Measurement mode	Spatial resolution
MWPCD	no	Transient	Local measurement, spatial information by mapping
QSSPC	yes	Transient or quasi-steady-state	Averaging over inductive coil area ( $\sim 10\text{cm}^2$ )
CDI/ILM	no	Steady-state	High, depending on camera resolution
Dynamic-ILM	no	Transient	High, depending on camera resolution
QSSPL	yes	Quasi-steady-state	Depending on diode and aperture mask
PLI	no	Steady-state	High, depending on camera resolution
TR-PLI, PLI	no	Transient	High, depending on dynamic-camera resolution
$\mu$ -PLM	no	Steady-state	Very high ( $\sim 1\mu\text{m}$ ), spatial information by mapping

**Table 1. Selected measurement methods for determining the minority carrier lifetime in crystalline silicon material for photovoltaic applications.**

more specifically, the microwave-detected photoconductance decay (MWPCD) methods, are very well-known and well-established techniques of measuring lifetimes in semiconductor materials. The first successful measurements date back to the late 1950s [3,4], and the technique has been the subject of continuous improvement and interest since that date (see [5–8] and references therein). In MWPCD measurements, excess carriers are generated by laser illumination and often combined with a background bias light. After switching off the external excitation, the time constant of the relaxation of the system back to equilibrium state is monitored. This is detected by the changing reflectance or absorption of a microwave signal. In practice, the length of the laser pulse and the laser wavelength may vary considerably between different measurement setups, which can influence the depth-dependent excess charge carrier profile that builds up in the sample under investigation and must be included in the analysis of the decay transient.

Another method for the determination of the minority carrier lifetime is the quasi-steady-state photoconductance (QSSPC) method, which was developed by Sinton and Cuevas in the 1990s [9]. Excess carriers are generated optically in the typical measurement setup by a polychromatic xenon flash light, and the resulting photoconductivity is determined via eddy current sensing by means of an inductively-coupled coil. The time-resolved illumination intensity is monitored by a reference solar cell, so that for a typical QSSPC measurement both the excess photoconductivity and the illumination intensity of the sample are measured simultaneously. Measurements

are relatively easy to perform, and a whole injection-dependent lifetime curve is obtained rapidly. The conversion of the measurement signal into absolute lifetimes requires knowledge of the carrier mobilities and the rate of photogeneration in the sample. Transient photoconductance measurements are also possible by adjusting the decay time of the excitation source; in this case, knowledge of the exact photogeneration rate is not mandatory. While maximum illumination intensities up to a few hundred suns allow for injection densities of up to  $10^{17}\text{cm}^{-3}$ , low-level injection measurements below  $\Delta n = 10^{13} -$

$10^{14}\text{cm}^{-3}$  are often prone to measurement artefacts such as carrier trapping [10] or depletion region modulation (DRM) [11] and have to be rejected or corrected.

Carrier density imaging/infrared lifetime mapping (CDI/ILM) is a camera-based measurement technique where the infrared absorption or emission of free carriers is detected [12,13]. It has, potentially, a high spatial resolution capability, but surface texture or lateral inhomogeneities of the optical properties may complicate the analysis. Furthermore, similar to the QSSPC technique, measurement artefacts such as trapping or DRM can be an issue in the low-level injection range. Typically, CDI/ILM is used in a steady-state mode by applying a lock-in technique with illumination switch on and off; recently, an extension which utilizes the transient parts of the switching sequence has been presented, the so-called dynamic-ILM [14]. The advantage of this technique is a calibration-free lifetime imaging of samples with arbitrary surface conditions and/or inhomogeneous doping concentration.

The electrical characterization techniques that probably experienced the most development and progress in the last five years are photoluminescence-based measurement methods. Electroluminescence [15] and photoluminescence imaging (PLI) [16] are two techniques that are currently widely used and allow for fast, spatially-resolved and high-resolution images of the minority carrier diffusion length and (effective) minority carrier lifetime, respectively. As PLI is in practice not affected by carrier trapping and similar measurement artefacts, the lifetime can in principle also

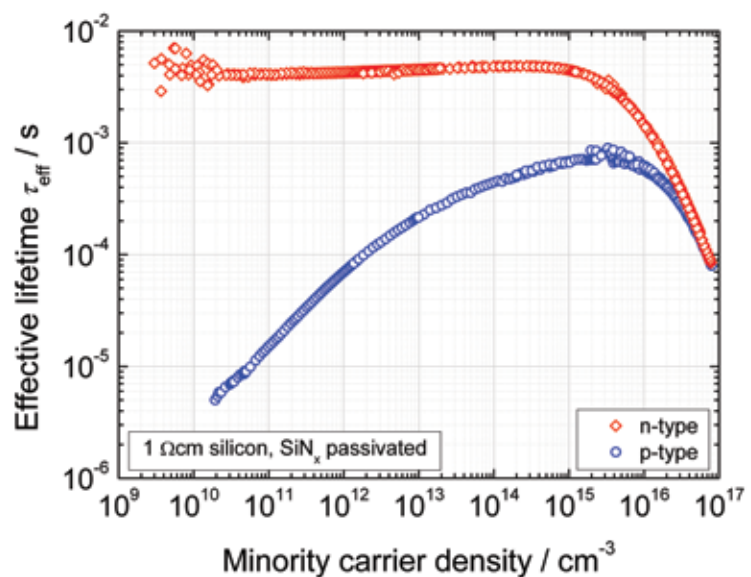


**Figure 2. Effective minority carrier lifetime curves of  $\text{SiN}_x$  surface-passivated  $1\Omega\text{cm}$  p-type and n-type float zone wafers. The lifetime has been determined by means of quasi-steady-state photoluminescence (QSSPL) measurements. The injection-dependence of the minority carrier lifetime can give valuable information about the lifetime-limiting mechanisms and dominating defect parameters.**

be measured reliably at very low excess carrier densities. PLI is a steady-state measurement technique, so, in order to get absolute lifetime data, a calibration of the detected photoluminescence is necessary. Different calibration methods exist – a popular approach is the calibration by integrating a QSSPC measurement [17]. Alternatively, a direct method to determine the lifetime from single PL images has also been presented [18].

“As PL-based measurements are in practice not affected by carrier trapping and similar measurement artefacts, the lifetime can in principle also be measured reliably at very low excess carrier densities.”

Apart from calibration, theoretical models for the coefficient of radiative emission and photon reabsorption are necessary, where optical properties of the sample have to be considered. In quasi-steady-state photoluminescence (QSSPL) measurements, the excitation source consists of a modulated laser or light-emitted diodes, so that the minority carrier lifetime is recorded in a broad range

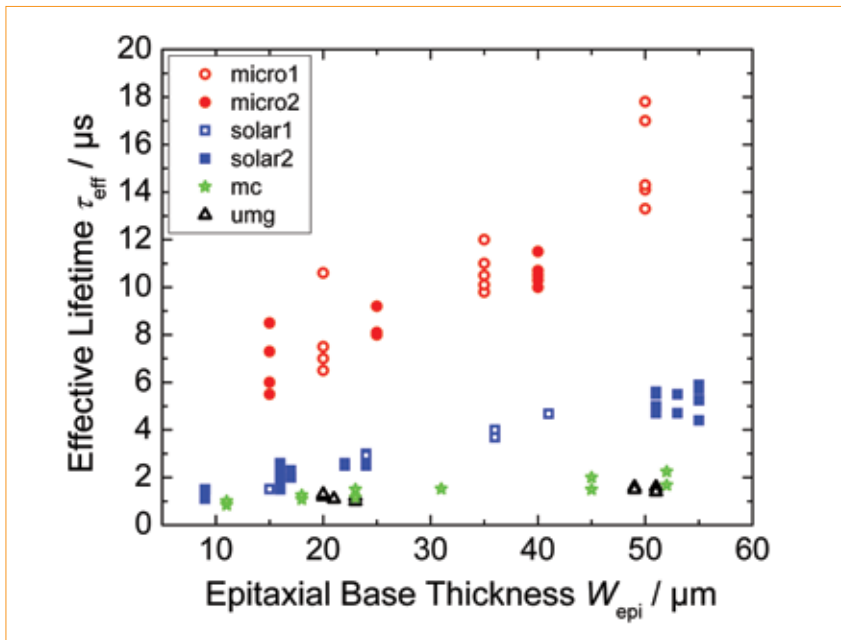
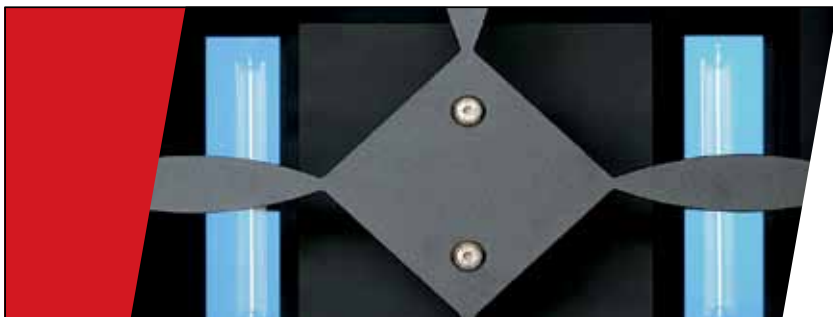


Figure 3. Effective lifetimes measured by means of microwave-detected photoconductance decay (MWPCD) on different crystalline silicon thin-film samples: monocrystalline substrates with microelectronic-grade epitaxial layers ('micro1' and 'micro2' – red circles); monocrystalline substrates with solar-grade epitaxial layers ('solar1' and 'solar2' – blue squares); standard multicrystalline substrates with solar-grade epitaxial layers ('mc' – green stars); and multicrystalline upgraded-metallurgical-grade silicon substrates with solar-grade epitaxial layers ('umg' – black triangles). The different groups exhibit clearly different effective lifetimes.

of excess carrier densities. Fig. 2 shows the lifetime curves of 1 $\Omega\text{cm}$  p- and n-type  $\text{SiN}_x$  surface-passivated float zone wafers.

Two promising PL-based characterization methods that have been developed recently are the  $\mu$ -PL lifetime mapping ( $\mu$ -PLM)



**PASAN**  
MEASUREMENT SYSTEMS

## Tested, Certified, Best in class – Pasan

### First class sun simulators

Pasan is the world reference for measurement equipment in the photovoltaic cell and module production. Our unrivalled technology in power measurement turns directly into your profit.



Solar award  
winner 2009, 2010.  
TüV Rheinland  
certified.

A member of Meyer Burger Group



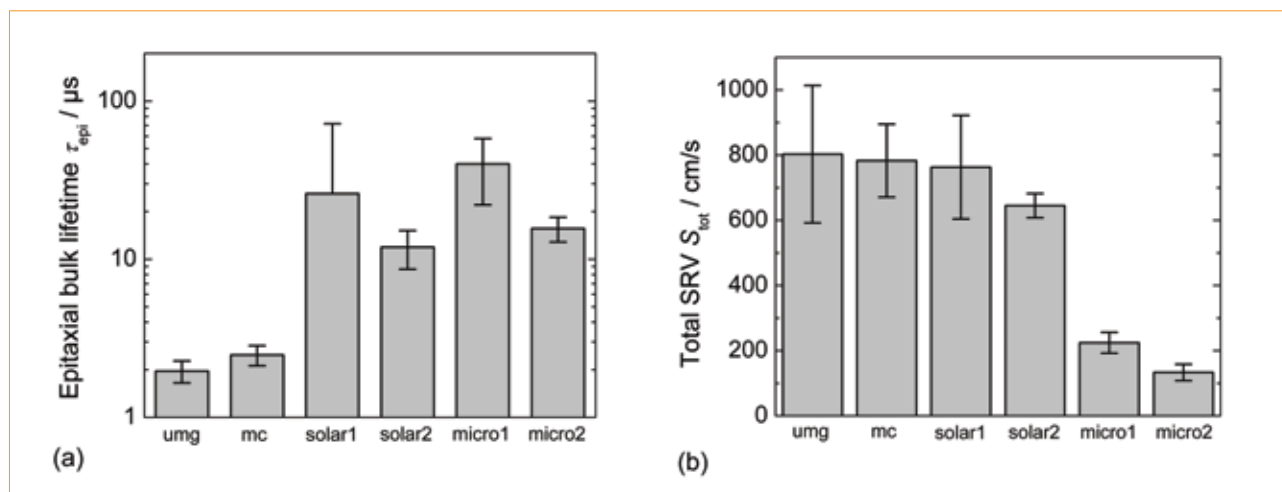


Figure 4. Epitaxial bulk lifetime (a) and total surface recombination velocity (SRV) (b) for different types of crystalline silicon thin-film material. A clear difference in the epitaxial lifetime can be observed between mono- and multicrystalline epitaxial layers, the former leading to epitaxial lifetimes in the range of a few microseconds, the latter leading to lifetimes well above 10 $\mu s$ . With regard to the total surface recombination velocity – which is equivalent to the effective interface recombination velocity as front surface recombination can be neglected due to high-quality silicon nitride front surface passivation – a significant difference between solar-grade ( $S_{tot} = 150\text{--}200\text{cm/s}$ ) and microelectronic-grade ( $S_{tot} = 650\text{--}800\text{cm/s}$ ) epitaxial samples is visible. This indicates the improvement potential for the processing of the solar-grade epitaxial layers. Error bars come from linear regression. Strictly speaking, the epitaxial lifetime of the sample set ‘solar1’ is not meaningful, as the error exceeds the mean value.

technique [19] and PLI techniques, which use a time dependence in the measurement, i.e. time-resolved photoluminescence imaging (TR-PLI) [20] and dynamic PLI [21]. The former enables quantitative lifetime measurements with a resolution of 1 $\mu m$  and can, for instance, be used for micro-PL spectroscopy, while the latter allows for fast and calibration-free lifetime images with a relatively basic measurement setup.

### Application to crystalline silicon thin-film material

Exemplarily, the determination of the minority carrier lifetime in crystalline silicon thin-film (cSiTF) material and its interpretation will be presented in the following. cSiTF solar cells are an attractive and promising alternative to bulk silicon solar cells, as the former require only a small fraction of costly high-purity silicon. They basically consist of a highly-doped p-type substrate, upon which a thin moderately-doped p-type layer is deposited epitaxially via chemical vapour deposition at elevated temperatures above 1000°C. After deposition of the epitaxial layer, which acts as the solar cell’s base, standard solar cell processing (emitter diffusion, front- and back-contact formation, anti-reflection coating) follows.

Measuring the lifetime in cSiTF material is challenging, because the two layers (epitaxial layer and substrate) cannot be separated physically and must therefore be measured together. (Some cSiTF concepts allow for a lift-off of the epitaxial layer from the substrate, which is not covered in this study.) In general, an influence of the substrate material is expected, as well as an influence from the interface between epitaxial layer and substrate. Microwave-detected

photoconductance decay (MWPCD) measurements are found to be well suited to deal with the particular requirements of cSiTF material. As has been shown in a detailed theoretical and empirical analysis [22], the effective minority carrier lifetime of cSiTF material can reliably be determined by means of short- or long-pulse MWPCD.

Fig. 3 shows the lifetimes of different types of cSiTF material using mono- and multicrystalline silicon as the substrate material. The epitaxial layers have been deposited in commercially-available microelectronic-grade chemical vapour deposition (CVD) reactors or in lab-type CVD reactors specifically designed for high-throughput photovoltaic applications. The epitaxial layers of the latter type are referred to as solar-grade cSiTF material. The measured effective lifetimes are strongly dependent on the thickness of the epitaxial base, which is mainly due to the impact of the interface. Different sample groups can clearly be distinguished by their effective lifetimes.

Note that the results in Fig. 3 include measurements by short- and by long-pulse excitation and that most measurements have been performed with laser wavelengths between 660 and 980nm (a few microcrystalline samples were additionally investigated by 350 and 532nm excitation). In agreement with the theoretical predictions [22], no systematic deviation between the different measurement conditions were observed for cSiTF material. Due to a relatively small signal-to-noise ratio, a high illumination intensity was chosen, leading to excess carrier densities in the range of 10<sup>15</sup> to 10<sup>18</sup>cm<sup>-3</sup> for the investigated

samples. Further studies in this area could investigate the actual injection level.

“The effective minority carrier lifetime could be determined on a wide range of different cSiTF materials successfully.”

With a single MWPCD measurement, the effective lifetime can be determined as demonstrated. In the case of a whole sample set of thin-film lifetime samples that differ only in their epitaxial layer thickness, even more information can be extracted. Under the stringent assumption that the investigated lifetime samples within one sample set have similar electrical and optical properties, the epitaxial bulk lifetime  $\tau_{epi}$  and the total recombination velocity  $S_{tot}$ , which encompasses the front surface recombination velocity ( $S_{front}$ ), the loss of minority charge carriers through a net current of minority charge carriers from the epitaxial base into the substrate (denoted by  $S_{BSF}$ ), and the recombination velocity at the interface ( $S_{int}$ ) via crystallographic defects and impurity atoms, can be separated according to Equation 3:

$$\frac{1}{\tau_{eff}} = \frac{1}{\tau_{epi}} + \frac{S_{front} + S_{BSF} + S_{int}}{W_{epi}} \quad (3)$$

Fig. 4 shows the results gathered by applying this analysis method to different cSiTF materials. Whereas no significant difference in the epitaxial bulk lifetime was observed between microelectronic-grade thin-film material and solar-grade epitaxial

layers deposited at Fraunhofer ISE, matters are different for the total surface recombination velocity, indicating the improvement potential for the processing of the solar-grade epitaxial layers.

Finally, note that  $S_{BSF}$  can in principle be calculated by applying the theory of high-low junctions [23]. When applied to thin-film solar cells, this translates into:

$$S_{BSF} = \frac{D_{substr}}{L_{substr}} \Phi \quad \text{where} \quad \Phi = \frac{N_{substr}}{N_{epi}} \quad (4)$$

where the diffusion coefficient and diffusion length of the minority charge carriers in the substrate are denoted by  $D_{substr}$  and  $L_{substr}$ , and the doping concentrations of the substrate and the epitaxial layer are denoted by  $N_{substr}$  and  $N_{epi}$ , respectively. For high doping concentrations, bandgap narrowing must be included in the calculation.

## Summary

This article has addressed the concept of minority carrier lifetime in photovoltaic silicon material. After the introduction of the fundamental relations, selected lifetime measurement methods have been presented, with results on crystalline silicon thin-film material showing the determination of effective lifetimes between 1 and 15  $\mu$ s. Additionally, under the assumption of negligible front-surface recombination and similar electrical and optical properties within one lifetime sample set, a method of separating the total recombination rate into epitaxial bulk lifetime, minority carrier loss through a net current of minority charge carriers from the epitaxial base into the substrate, and recombination at the interface has been proposed.

## References

- [1] Trupke, T. et al. 2004, "Effective excess carrier lifetimes exceeding 100 milliseconds in float zone silicon determined from photoluminescence", *Proc. 19th EU PVSEC*, Paris, France, pp. 758–61.
- [2] Nagel, H., Berge, C. & Aberle, A.G. 1999, "Generalized analysis of quasi-steady-state and quasi-transient measurements of carrier lifetimes in semiconductors", *Journal of Applied Physics*, Vol. 86, pp. 6218–21.
- [3] Ramsa, A.P., Jacobs, H. & Brand, F.A. 1959, "Microwave techniques in measurement of lifetime in germanium", *Journal of Applied Physics*, Vol. 30, pp. 1054–60.
- [4] Jacobs, H., Ramsa, A.P. & Brand, F.A. 1960, "Further consideration of bulk lifetime measurement with a microwave electrodeless technique", *Proc. Institute of Radio Engineers*, Vol. 48, pp. 229–33.
- [5] Kunst, M. & Beck, G. 1986, "The study of charge carrier kinetics in semiconductors by microwave conductivity measurements", *Journal of Applied Physics*, Vol. 60, pp. 3558–66.
- [6] Schöfthaler, M. & Brendel, R. 1995, "Sensitivity and transient response of microwave reflection measurements", *Journal of Applied Physics*, Vol. 77, pp. 3162–73.
- [7] Ogita, Y.I. 1996, "Bulk lifetime and surface recombination velocity measurement method in semiconductor wafers", *Journal of Applied Physics*, Vol. 79, pp. 6954–60.
- [8] Ahrenkiel, R.K. & Johnston, S.W. 2008, "Lifetime analysis of silicon solar cells by microwave reflection", *Solar Energy Materials and Solar Cells*, Vol. 92, pp. 830–5.
- [9] Sinton, R.A. & Cuevas, A. 1996, "Contactless determination of current-voltage characteristics and minority-carrier lifetimes in semiconductors from quasi-steady-state photoconductance data", *Applied Physics Letters*, Vol. 69, pp. 2510–2.
- [10] Macdonald, D. & Cuevas, A. 1999, "Trapping of minority carriers in multicrystalline silicon", *Applied Physics Letters*, Vol. 74, pp. 1710–2.
- [11] Bail, M., Schulz, M. & Brendel, R. 2003, "Space-charge region-dominated steady-state photoconductance in low-lifetime Si wafers", *Applied Physics Letters*, Vol. 82, pp. 757–9.
- [12] Bail, M. et al. 2000, "Lifetime mapping of Si wafers by an infrared camera [for solar cell production]", *Proc. 28th IEEE PVSC*, Anchorage, Alaska, USA, pp. 99–103.
- [13] Riepe, S. et al. 2001, "Carrier density and lifetime imaging of silicon wafers by infrared lock-in thermography", *Proc. 17th EU PVSEC*, Munich, Germany, pp. 1597–9.
- [14] Ramspeck, K. et al 2008, "Dynamic carrier lifetime imaging of silicon wafers using an infrared-camera-based approach", *Applied Physics Letters*, Vol. 93, pp. 102104–1–3.
- [15] Fuyuki, T. et al 2005, "Photographic surveying of minority carrier diffusion length in polycrystalline silicon solar cells by electroluminescence", *Applied Physics Letters*, Vol. 86, pp. 262108–1–3.
- [16] Trupke, T. et al 2006, "Photoluminescence imaging of silicon wafers", *Applied Physics Letters*, Vol. 89, pp. 044107–1–3.
- [17] Herlufsen, S. et al 2008, "Photoconductive-calibrated photoluminescence lifetime imaging of crystalline silicon", *physica status solidi RRL*, Vol. 2, pp. 245–7.
- [18] Giesecke, J.A., Kasemann, M. & Warta, W. 2009, "Determination of local minority carrier diffusion lengths in crystalline silicon from luminescence images", *Journal of Applied Physics*, Vol. 106, pp. 014907–1–8.
- [19] Gundel, P. et al 2010, "Quantitative carrier lifetime measurement with micron resolution", *Journal of Applied Physics*, Vol. 108, pp. 033705–1–7.
- [20] Kiliani, D. et al. 2010, "Time resolved photoluminescence imaging for carrier lifetime mapping of silicon wafers", *Proc. 25th EU PVSEC*, Valencia, Spain [in print].
- [21] Herlufsen, S. et al. 2010, "Dynamic lifetime imaging based on photoluminescence measurements", *Proc. 25th EU PVSEC*, Valencia, Spain [in print].
- [22] Walter, D. et al 2010, "Determining the minority carrier lifetime in epitaxial silicon layers by microwave-detected photoconductivity measurements", *Proc. 25th EU PVSEC*, Valencia, Spain [in print].
- [23] Godlewski, M.P., Baraona, C.R. & Brandhorst, Jr., H.W. 1973, "Low-high junction theory applied to solar cells", *Proc. 10th IEEE PVSC*, Palo Alto, California, USA, pp. 40–9.

## About the Author



**Philipp Rosenits** studied physics at the Universidad de Costa Rica and the University of Freiburg, where he received his degree in physics in 2007.

His diploma thesis, which he accomplished at the Australian National University and the Fraunhofer ISE, was about the characterization of electrically active defects in silicon. He is currently finishing his Ph.D. thesis, which deals with the electrical characterization of crystalline silicon thin-film material. Besides science, he is also interested in intellectual property rights and patents.

## Enquiries

Fraunhofer Institute for Solar Energy Systems (ISE)  
Heidenhofstr. 2  
79110 Freiburg  
Germany  
Tel: +49 761 4588 5269  
Fax: +49 761 4588 9250  
Email: philipp.rosenits@ise.fraunhofer.de